Review of the Low-Temperature Acoustic Properties of Water, Aqueous Solutions, Lipids, and Soft Biological Tissues

Suzi Liang, Bradley E. Treeby, and Eleanor Martin

***Abstract*—Existing data on the acoustic properties of low-temperature biological materials is limited and widely dispersed across fields. This makes it difficult to employ this information in the development of ultrasound applications in the medical field, such as cryosurgery and rewarming of cryopreserved tissues. In this review, the low-temperature acoustic properties of biological materials, and the measurement methods used to acquire them were collected from a range of scientific fields. The measurements were reviewed from the acoustic setup to thermal methodologies for samples preparation, temperature monitoring, and system insulation. The collected data contain the longitudinal and shear velocity, and attenuation coefficient of biological soft tissues and biologically relevant substances—water, aqueous solutions, and lipids—in the temperature range down to −50 °C and in the frequency range from 108 kHz to 25 MHz. The multiple reflection method (MRM) was found to be the preferred method for low-temperature samples, with a buffer rod inserted between the transducer and sample to avoid direct contact. Longitudinal velocity changes are observed through the phase transition zone, which is sharp in pure water, and occurs more slowly and at lower temperatures with added solutes. Lipids show longer transition zones with smaller sound velocity changes; with the longitudinal velocity changes observed during phase transition in tissues lying between these two extremes. More general conclusions on the shear velocity and attenuation coefficient at low-temperatures are restricted by the limited data. This review enhance knowledge guiding for further development of ultrasound applications in low-temperature biomedical fields, and may help to increase the precision and standardization of low-temperature acoustic property measurements.**

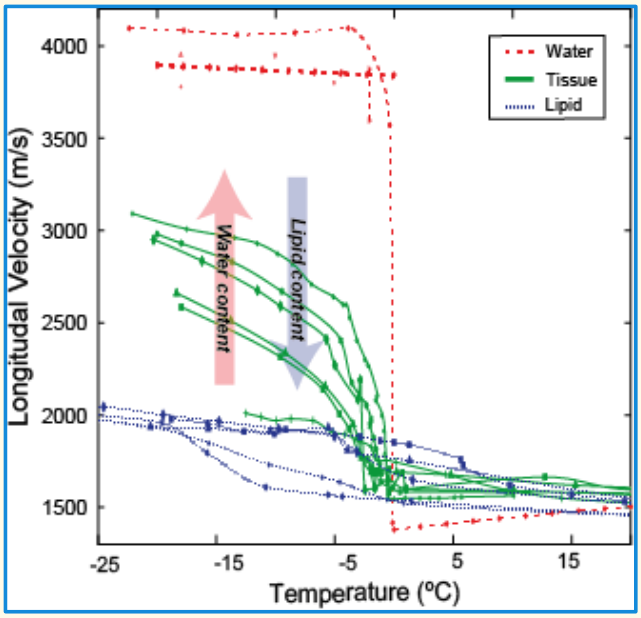

***Index Terms*— Acoustic properties, attenuation coefficient, low-temperature, measurement methods, sound velocity, ultrasonic material characterization.**

I. Introduction

THE way ultrasonic waves propagate through materials is determined by their acoustic properties, specifically the sound velocity and attenuation coefficient. These properties are determined by the materials themselves [1], [2]. By tracking changes in acoustic properties, variations in materials due to changing environmental factors can be quantified [3]. This principle is applied in many different fields, including nondestructive testing (NDT) [4], subharmonic-aided pressure estimation (SHAPE) [5], [6], [7], [8], medical ultrasound diagnosis [9], and underwater acoustic detection [10].

Much of the current research on the characterization of the acoustic properties of materials and acoustic characterization of the materials themselves has been conducted at temperatures above 0 °C [11], [12], [13], [14], with less emphasis on temperatures below 0 °C [15]. Additionally, existing studies of properties at low-temperature are spread across various fields, including seismology [16], [17], [18], glaciology [19], [20], and the food industry [15], [19], [20]. In the field of seismology, acoustic properties of water-ice have been measured in order to monitor the structure, length, and temperature of ice sheets [16], [17], [18]. Similarly, in glaciology, variations in acoustic properties of ice have been investigated as a function of salinity for monitoring sea ice sheets [19], [20]. In the food

Manuscript received 2 February 2024; accepted 18 March 2024. Date of publication 26 March 2024; date of current version 13 May 2024. This work was supported in part by the UK Research and Innovation (UKRI) Future Leaders Fellowship under Grant MR/T019166/1, in part by the Wellcome/Engineering and Physical Sciences Research Council (EPSRC) Center for Interventional and Surgical Sciences (WEISS) under Grant 203145Z/16/Z, and in part by the EPSRC Center for Doctoral Training (CDT) in Intelligent, Integrated Imaging in Healthcare (i4health). *(Corresponding author: Suzi Liang.)*

Suzi Liang and Eleanor Martin are with the Department of Medical Physics and Biomedical Engineering and the Wellcome/EPSRC Center for Interventional and Surgical Sciences, University College London, WC1E 6BT London, U.K. (e-mail: rmapsl0@ucl.ac.uk).

Bradley E. Treeby is with the Department of Medical Physics and Biomedical Engineering, University College London, WC1E 6BT London, U.K.

Digital Object Identifier 10.1109/TUFFC.2024.3381451

Highlights

- **Low-temperature acoustic properties of biological materials and measurement methods are collected from a range of scientific fields and reviewed as a foundation for development of new applications of medical ultrasound.**
- **Longitudinal velocity changes correspond to phase transition, which is sharp in pure water, moving to lower temperatures with added solutes. Lipids show longer transition zones with smaller velocity change, with tissues in between.**
- **This review provides a useful resource, collecting knowledge crucial to the development of medical applications of ultrasound such as rewarming of cryopreserved tissue and cryosurgery and may aid in standardization of measurements.**

industry, the acoustic properties of food [15], [19], [20] as a function of temperature below 0 °C have been measured to monitor ice crystallization in food during freezing and thawing.

The spread of measured data across fields constrains our understanding of the acoustic properties of materials in the low-temperature range. However, application of the knowledge to other fields may aid the development of new technologies, for example, in medical applications such as cryosurgery and cryopreservation.

Cryosurgery is a procedure in which malignant tumor tissue is destroyed by freezing [21]. During cryosurgery, ultrasonic imaging can be used to provide real-time monitoring of location and extent of frozen tissue [22]. In practice, bulk variations of acoustic properties are often used to confirm tissue freezing has occurred [23], rather than using temperature-dependent acoustic properties to perform continuous monitoring during freezing.

Cryopreservation is a technique used to maintain the viability of cells, tissues, and organs by freezing with the addition of cryoprotective agents [22]. In future, this technology could be used to bank organs: that is to preserve cells, tissues, and organs at low-temperature for extended periods, and rewarm them when needed [24]. One of the biggest challenges in achieving this is that only small volumes of tissue can be rewarmed without damage [25]. For larger volumes of tissue, rewarming methods that provide uniform and rapid heating are necessary. Ultrasound has demonstrated potential in this case [26], [27].

For the development of both cryosurgery and cryopreservation applications, it is important to understand the acoustic properties of biological tissues and their dependence on temperature during freezing and thawing. For cryosurgery, this knowledge could improve the accuracy of ultrasound monitoring during cryosurgery. For rewarming tissues after cryopreservation, this knowledge is required for planning the delivery of energy for effective rewarming of large volumes of tissues using ultrasound.

The acoustic properties of tissues during freezing are related to the composition and ratio of their constituent components, such as water, lipids [28], and proteins [29]. Furthermore, the water present in tissues is mixed with organic and inorganic compounds [30], [31]. Changes in the acoustic properties of water as a function of solute concentrations during freezing, are therefore also significant.

In this review, we aim to gather information on the low-temperature acoustic properties of biological tissues and their main components, including water, aqueous solutions, and lipids. Specifically, the longitudinal and shear velocity, and attenuation coefficients measured at temperatures below 0 °C, and in the 100 kHz to MHz frequency range. A literature search was performed using these search terms with a variety of search engines. These data are currently spread across a diverse range of fields and have not previously been collected and presented together. There is also a lack of systematic investigation of the dependence of the properties of materials with temperature across frequencies, and a limited range of sample materials. The methods used for those measurements, including system setup and calculation methods, are also reviewed. Additionally, the challenges and considerations involved in designing measurements when the sample is below 0 °C, including sample preparation (freezing protocol), temperature monitoring, and thermal insulation, are discussed. Collating information about measurement methods employed across fields will help to improve understanding of variations and uncertainties in measured results. This may serve as a reference for the design of future methods and systems for measurement of low-temperature acoustic properties.

II. Methods for Measuring Low-Temperature Samples

In this section, we first define the relevant acoustic properties and introduce the general setup and calculation methods used to acquire the data presented in this review. The methods used for low-temperature acoustic property measurement are discussed in terms of both from the acoustic and thermal considerations.

A. Definition of Acoustic Properties

1) Sound Velocity and Speed: Sound velocity, a vector quantity, combines the scalar speed of wave propagation with its direction of propagation [32]. Here, we present data on both longitudinal velocity (velocity of compressional waves and propagating in the direction of particle motion), and shear velocity (transverse waves propagating perpendicular to direction of particle motion) [33].

2) Group Velocity: The frequency-independent velocity, group velocity, is an estimate of the overall traveling velocity of a waveform packet (or pulse). The group velocity is usually calculated by a time-of-flight (TOF) method, whose principle

is to calculate the velocity in the time-domain based on time delay between waveforms traveling a known distance [34]. The time delay can be derived using a range of time-picking criteria, for example, using the mid points or center of mass of the wave packet [35], the location of the waveform peak [36], or the start point of the waveform (waveform onset) [37], which may also be described as the signal velocity [38], [39].

3) Phase Velocity: The frequency-dependent velocity, phase velocity, or dispersion, is an estimate of the velocity at which individual frequency components travel. The phase velocity is calculated in the frequency domain by comparing unwrapped phase differences between the components of two waveform spectra, one acquired in reference medium only and one acquired after propagation through a sample [40].

4) Attenuation Coefficient: During waveform propagation in material, the energy of the waveform decreases, through either intrinsic or extrinsic factors [1]. Intrinsic attenuation arises from scattering and absorption (i.e., conversion of energy to heat), which is a property of the material itself, and is frequency dependent [9]. On the other hand, the extrinsic attenuation arises from factors related to the propagation of the wave, for example, beam divergence, edge effects, or surface losses. In order to measure the intrinsic attenuation coefficient, the effects of extrinsic factors must be excluded.

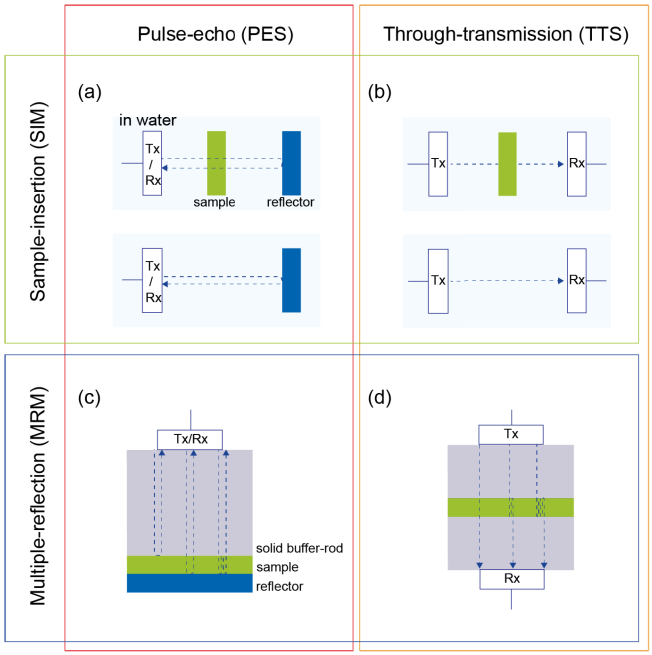

Fig. 1. Acoustic properties measurement system using different combinations of two system setups: PES and TTS, and two calculation methods: SIM and MRM. The diagrams show the combination of (a) PES and SIM, (b) TTS and SIM, (c) PES and MRM, and (d) TTS and MRM. The abbreviations of Tx and Rx in the figures denote the transmission and receive, respectively.

B. Measurement Methods

When it comes to measuring the acoustic properties, the essential components are: a pulser/receiver (to drive the transducer), an oscilloscope (to sample the waveform), and acoustic devices (to transmit and receive signals). The setup can be categorized based on the number of acoustic devices used, as either a pulse-echo setup (PES) or through-transmission setup (TTS). PES uses a single transducer to transmit pulses and receive waveforms [41] while TTS uses separate transducers either side of the sample to transmit pulses and receive waveforms. Both PES and TTS are acoustically equivalent for the measurement of group velocity and attenuation coefficient. For phase velocity, however, TTS is used rather than PES [40], [42], as phase changes during reflection and scattering complicate the measurement.

Acoustic properties can be calculated using two methods, respectively, with or without the use of a reference medium. The sample-insertion method (SIM) [4], involves comparing waveforms acquired in a reference medium to those acquired with the sample in place. The most commonly used reference medium when making measurements at ambient temperatures is distilled or deionized water, for which the acoustic properties are well characterized as a function of frequency, pressure, and temperature [43], [44], [45], [46]. However, water is unsuitable as a reference medium for the measurement of acoustic properties below 0 °C due to freezing. Alternative liquids with lower freezing points are viable substitutes for such low-temperature acoustic properties measurements.

Another measurement method is the multiple reflection method (MRM) [47], [48], [49], [50], [51], in which the physical relationship of echoes reflected by the samples are analyzed to calculate sound velocities and attenuation coefficients. Rather than a reference medium, the MRM setup compromises a solid buffer rod inserted between the transducer and sample with the addition of a coupling agent, such as ultrasonic gel. Polymethyl methacrylate (PMMA), quartz glass, aluminum, and stainless steel are common buffer rod materials, due to their relatively low attenuation, temperature stability, and chemical resistance [47]. The diagram in Fig. 1 shows the four combinations of system setups and calculation methods commonly used for measuring acoustic properties [4].

C. Measurement Methods for Sample Below 0 °C

In this section, we review the methods employed in the studies collected here in terms of the acoustic and thermal considerations. The measurement conditions during these studies are listed in Table I. The samples characterized include water, aqueous solutions (mainly NaCl), animal fat and vegetable oil, and biological tissues. The measurement frequencies ranged from 108 kHz to 25 MHz, and measurements were made at temperatures down to −50 °C. Note that the longitudinal and shear velocity of the Greenland and Antarctic ice samples were sourced from a review paper [17], which did not give details of the specific measurement conditions, and is therefore not listed in Table I.

1) Acoustic System Setup and Calculation Method: Different combination of PES or TTS measurement methods with SIM or MRM calculation methods can be used to obtain the acoustic properties (Fig. 1). Both PES and TTS methods were employed in the studies collected here, as listed in Table II. Normally, two transducers are used in TTS, one to transmit a pulse and the other to receive a signal. However, in one particular study characterizing the bubbly and bubble-free ice [53] [study index (2)], six receivers were employed to simultaneously record the propagated waveforms. These receivers were positioned at the same distance, in a line perpendicular to the direction of propagation of the transmitted

TABLE I
MEASURED CONDITIONS FOR LOW-TEMPERATURE ACOUSTIC PROPERTIES

Study index	Sample	Acoustic property	Frequency (MHz)	Temperature (°C)
1 [52]	Distilled-water ice	c_l	2.5	$[-25, 0]$
2 [53]	Bubble-free ice	c_l, c_s	0.108	$[-20, 0]$
3 [16]	Bubbly ice Bubble-free ice	c_l	5	-18
4 [54]	Pure-water ice	c_l, c_s	5	-26
5 [55]	Fresh water 0.3% (w/w) NaCl solution	c_l, c_s	1	$[-30, 0]$
6 [56]	2% (w/w) NaCl solution	c_l	2	$[-15, 20]$
7 [57]	1-4% (w/w) NaCl solution	c_l	N/A	$[-20, 20]$
8 [58]	50% (w/w) NaCl solution	c_l	$[0.219, 0.732]$	$[-20, 18]$
9 [59, 20, 60]	Fat and oil Tissue	c_l	2.25	$[-50, 100]$ $[-20, 40]$
10 [19]	Bovine skeletal muscle	α	$[1, 7]$	-20, 0, 20
11 [61]	Bubbly ice Bubble-free ice	c_l, α	$[7, 15]$	-10 -5
12 [62]	Pure-water ice	c_l, α	25	$[-2, 0]$
13 [63]	Orange juice	c_l, c_s, α	5	$[-50, 0]$

c_l: Longitudinal velocity, c_s: Shear velocity, and α: Attenuation coefficient.

TABLE II
ACOUSTIC SETUP AND CALCULATION METHOD USED FOR TABLE I

Study index	Set-up	Velocity calculation	Attenuation coefficient calculation	Coupling medium
1 [52]	PES	TOF	N/A	Plexiglas delay line
2 [53]	TTS (One device to transmit and six to receive)	TOF (start)	N/A	N/A
3 [16]	PES	TOF	N/A	Thin film of water (< 0.1 mm)
4 [54]	PES	TOF	N/A	Aluminium plate
5 [55]	TTS	TOF (peak)	N/A	Plastic film
6 [56]	TTS	TOF (start)	N/A	N/A
7 [57]	TTS	TOF (peak)	N/A	Thin glass window
8 [58]	TTS	TOF	N/A	N/A
9 [59, 20, 60]	TTS	TOF	N/A	N/A
10 [19]	TTS	N/A	SIM	Glass and perspex
11 [61]	PES	TOF (peak)	MRM	Aluminium plate
12 [62]	PES	TOF	MRM	Fused-quartz thin window
13 [63]	PES	TOF	MRM	Panametrics commercial delay line

PES: Pulse-echo set-up, TTS: Through-transmission set-up, TOF: Time-of-flight, SIM: Sample-insertion Method, and MRM: Multiple-reflection Method.

wave. In this case, the measured sample size was significantly larger than those in other studies reviewed, with a diameter of 1.85 m and a depth of 1 m, in contrast to the sample sizes in other studies, which were on the scale of centimeters or millimeters. The substantial size of the sample leads to increased measurement uncertainty and complexity, mainly due to greater temperature variations and diminished sample homogeneity caused by the presence of bubbles and cracks. Furthermore, the larger sample size tends to decrease the signal-noise-ratio (SNR) owing to a longer propagation path. Nonetheless, these challenges mirror real-world conditions, making the findings more applicable to real-world scenarios. Multiple receivers may have been used to acquire several measurements over different paths to help reduce uncertainty in the measurements.

TOF was used to obtain sound velocity by all studies by picking either the start point [53], [56] or the peak value [55], [57], [61] of the waveform as the reference for time-delay calculation. Since all the studies used TOF, the velocities measured are group velocities, rather than the frequency dependent phase velocity. Therefore, where longitudinal velocity is used in this article, it is referring to group velocity. Both the system setup and the calculation methods employed are consistent across the measurements of both longitudinal and shear waves.

TABLE III
FREEZING PROTOCOL, THERMAL MONITORING, AND MAINTENANCE USED FOR TABLE I

Study index	Freezing protocol	Temperature sensor location	Thermal maintenance
1 [52]	Freeze by one-sided contacting	Sample surface (near to transducer)	Short acquisition time (2 sec)
2 [53]	Freeze by one-sided contacting	Near transducer	Stored in cryostatic path
3 [16]	N/A	Sample surface (near to transducer)	Short acquisition time (1 min)
4 [54]	Freeze by cooling-air surrounding	N/A	N/A
5 [55]	Freeze by cooling-air surrounding	Near transducer	Stored in cryostatic path
6 [56]	N/A	Inside sample	Stored in cryostatic path
7 [57]	Freeze by cooling-air surrounding	Inside sample	Stored in cryostatic path
8 [58]	Freeze by cooling-air surrounding	Inside sample	Stored in cryostatic path
9 [59, 20, 60]	N/A	N/A	Stored in cryostatic path
10 [19]	N/A	Inside sample	Thermal-insulation setting (circulating fluid through a wrapped jacket around sample)
11 [61]	Freeze by one-sided contacting	N/A	N/A
12 [62]	N/A	Near transducer	N/A
13 [63]	Freeze by cooling-air surrounding	Inside sample	N/A

For calculation of attenuation coefficient, three among four studies used MRM, while only one chose SIM. The reference medium used in SIM by Shore et al. [19] was ethyl alcohol rather than distilled water, which has a freezing point of −114 °C, below the sample temperatures of −20 °C [64]. The studies which used MRM, employed solid buffer rod materials ranging from aluminum plate [61], glass and perspex [19], fused-quartz, and a commercial delay line for which the material is not specified [63]. One function of the buffer rods used in low-temperature measurements is to prevent direct contact between the transducer and the frozen sample for protection. This precaution is necessary because unlike the widely studied performance of transducers at high-temperature [65], [66], their performance at low-temperatures is not well characterized.

In addition, the buffer rod acts as a delay line to prevent waveform mixing from the transmitted signal and returning echoes, and to ensure that the sample is positioned within the far-field of the transducer. The waveform in the far-field is regarded as more stable and can be approximated as a plane wave [67]. For a plane piston transducer, when transducer size is far larger than the wavelength, the transition distance between the near and far-field can be calculated as [68]

$$z \approx \frac{a^2}{\lambda} = a^2 \frac{f}{c} \tag{1}$$

where a represents the transducer radius, λ is the wavelength, c is the sound velocity in the medium, and f is the frequency used in the measurements. The center frequency of the transducer reported by the original papers is used for the near-field distance calculation. For the studies listed in Table I, the positioning of the sample varies between the near and far fields. In some studies, either no buffer medium was inserted or a thin film was used only to separate transducer and sample [studies (2, 3, 5, 6, 7, 8, 9, 12)], so the sample lies within the near field. A thin film is defined as a material layer of a few micrometers [69]. For studies [7, 12], which use a thin window made of glass or fused quartz, we regard them as a thin film as well, where the exact thickness is not given. In studies [1, 4, 10, 11, 13], media thicker than a few millimeters were chosen. However, it is unclear whether the samples were in the near or far field [study index (1, 11)]. For instance, in study index (1), the last axial maximum is calculated to be at 3.62 cm using the frequency of 2.5 MHz and transducer diameter of 1.25 cm, and a longitudinal velocity in the plexiglas medium of 2700 m/s [70]. However, the thickness of the plexiglas was not provided. Some other key information is missing in other studies, such as the transducer diameter [study index (10, 13)].

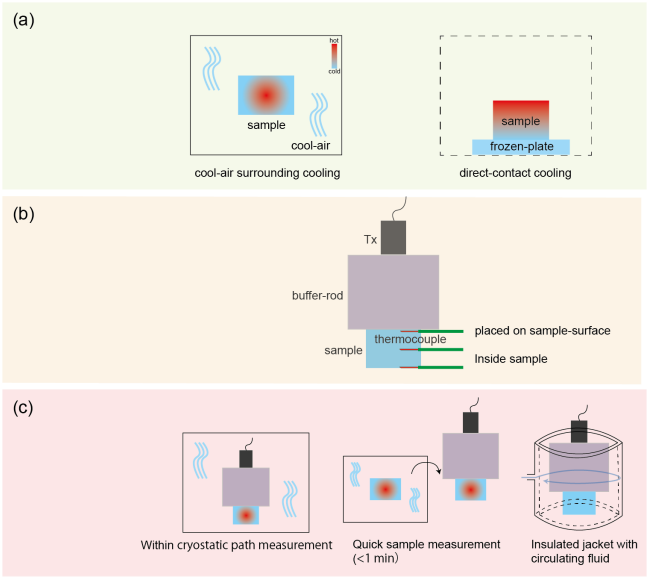

Fig. 2. Thermal conditions employed by the low-temperature acoustic property measurements in this study. (a) Freezing methods. (b) Temperature monitoring by different placements of the thermocouples. (c) Temperature maintenance.

2) Freezing Protocol, Temperature Monitoring, and Maintenance: To obtain high-quality measurements, the sample state and the environmental conditions must be well controlled. For low-temperature samples, the freezing protocol, temperature monitoring, and thermal maintenance are critical factors. Table III details and Fig. 2 illustrates the preparation,

monitoring, and maintenance methods employed by the studies listed in Table I.

Heat transfer between materials primarily occurs by three mechanisms: conduction, convection, and radiation [71]. The freezing methods utilized in the studies listed in Table I can be categorized into two groups based on these transfer mechanisms, including the one-sided contacting and cooling-air surrounding freeze [Fig. 2(a)]. In some studies [1, 2, 11], samples are frozen by direct contact with a cold surface. In this case, heat is transferred from the samples to the colder material by conduction. This process leads to one side of the sample being colder than the other, as heat is conducted away from the contact surface. Conversely, in other studies [4, 5, 7, 8, 13], the samples were frozen in a commercial refrigerator [55], [72] or freezer [58], [63]. Here, heat is transferred from the samples to the surrounding cooling-air by conduction and convection [73]. This method leads to a different temperature distribution across the samples compared to one-sided cooling, with the outer surface of the sample cooling faster than the center.

The rationale behind the selected cooling method for each study varies, encompassing practical considerations, and the specific objectives of the experiment. The cool-air surrounding method is readily accessible, due to the common use of the commercial freezer and refrigerators in laboratories. Stirling engine-type freezers which work by conducting heat away from a plate on which the sample is placed are another practical option since they can be relatively compact and cryogen free. While both cooling methods allow for the dynamical monitoring of velocity changes during freezing or thawing cycles, the one-side cooling method may be chosen when directional freezing is desired [74], [75], [76].

To establish the temperature dependence of the acoustic properties, the temperature of the sample must be measured during measurement. Several types of temperature sensors have been used to monitor the temperature of samples during freezing [77], including the semiconductor-based sensors [53], T-types thermocouples [52], [57], and K-type thermocouples [16], [62]. The studies mentioned all used a single temperature sensor, and the recorded temperature was considered the core temperature of the sample. Temperature sensor accuracy was reported only in the study of 2% (w/w) NaCl solution [56], where it was within ±0.1 °C. The positions of the temperature sensors in these studies varied [Fig. 2(b)], being placed on the sample surface closest to the transducer [16], [52], attached near the transducer [53], or inserted inside the sample [19], [55], [56], [57], [58], [62], [63]. Thermocouples placed inside the sample were embedded before freezing.

The temperature recorded by the thermocouples is influenced by the cooling method and the sensor location, as discussed by Sigfusson [52]. If the sample is frozen via contacting to a freezing plate, and the thermocouples was positioned on the sample surface in contact with the freezing plate, the lowest temperature of the sample is recorded. In this case, the temperature gradient between the top and bottom surface should be considered, and may depend on freezer performance, sample volume, and material properties, such as effective heat capacity [78]. Alternatively, when freezing is facilitated through cooling-air, such as in the commercial freezer, the temperature gradients between the outer and inner parts of the sample should instead be considered.

Maintenance of sample temperature during measurement is also critical to ensure the precision of the results, with three methods used by the reviewed studies [Fig. 2(c)]. Completing the measurement process in a short period of time is one method used to prevent heat gain during experiments. For example, in two studies, the frozen samples were removed from the freezer for 2 s [52] and 1 min [16], respectively, to complete the measurement, during which time no temperature change was observed. Completing the measurement within the cryostatic path without moving the sample is another method used to maintain temperature, which has been widely adopted [20], [53], [55], [56], [57], [58], [59], [60]. Additionally, thermally insulated setups have been used to store the sample during measurement. Shore et al. [19] placed sample outside the freezer in a container wrapped with a jacket of circulating fluid, maintaining the sample temperature error within a margin of ±0.5 °C during measurements.

III. Acoustic Properties at Low Temperatures

The acoustic properties of frozen samples measured in different studies are collected here. They are classified by materials type: pure water, aqueous solutions, lipids, and soft biological tissues, and by acoustic quantity: longitudinal and shear velocity, and attenuation coefficient. All figures in this review were generated by replotting data from the original studies, and plotting trends described by equations given in the original articles. When the data had not previously been described mathematically, curves were fit here using piecewise cubic Hermite interpolation to illustrate the trend [79], with "pchip" and "ppval" functions in MATLAB (The Mathworks Inc., Natick, USA).

A. Longitudinal Velocity of Pure Water

Water, serving as a fundamental component for all biological life forms, plays a crucial role in various physiological processes. Measurements of the longitudinal velocity of water-to-ice during freezing and thawing are presented in Fig. 3. The phase transition from water to ice is marked by a notable increase in longitudinal velocity, with a dramatic 189% increase in velocity during the transition in distilled water. The longitudinal velocity of distilled water increases from 1417 m/s for liquid water at 0 °C to 4095 m/s for solid ice at −3 °C [43], [52].

The trends in sound velocities with temperature in water and ice appear to diverge: the velocity of water is known to increase with temperature [80], [81], and here a positive slope of approximately 5.0 m/(s·°C) was observed in the distilled water measurements [study index (1)] [43], [52]. However, the trend in ice velocities within the same study is not clearly defined. In a contrasting observation, measurements from bubble-free ice [study index (2)] [53] indicated a negative slope of 2.8 m/(s·°C). Due to the constraints of the available data, a conclusive comparison between the velocity trends of ice and water cannot be made.

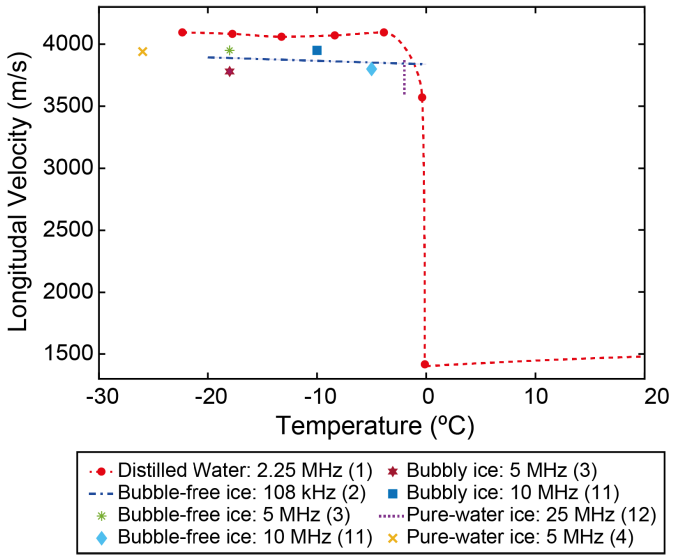

Fig. 3. Longitudinal velocity versus temperature of water and ice. The sample materials and their measured frequencies are described in the legend; the number in brackets is the study index used in Tables I–III Markers in the figure represent data sourced from original studies. Fit curves for study index above 0 °C (1) and study index (2) were based on equations from the original studies. For study index (1) below 0 °C, the curve was derived using piecewise cubic Hermite interpolation [79].

Comparison of longitudinal velocity of water-ice across different water types and measurement conditions reveals variations as high as 7.7% in measurements taken at the same temperature. The longitudinal velocity of water-ice, including bubbly and bubble-free water, distilled water and pure water, spans from 3595 to 4095 m/s measured in the temperature range of −26 °C to 0 °C. The maximum observed difference between measurements of different samples acquired at the same temperature at −18 °C, was between bubbly ice at 5 MHz and distilled water at 2.25 MHz with velocities of 3780 and 4083 m/s. To rationalize these differences, we should consider that several factors can influence the measurements.

1) *Impurities:*
Prior research indicates that a 1.5 p.p.m. increase in density results in a 1 p.p.m. increase in velocity [82]. The purity levels of distilled water and pure water, where distilled water is a type of pure water [83], may differ based on the purification process used in the studies. Differences arising between different types of nonsalt-water samples due to impurities are likely to be small.
2) *Bubbles Quantity and Size:*
Regardless of water purity level, variations in bubble quantity and size within ice samples should not be ignored. As noted by Thuraisingham [84], the volume concentrations and radius of bubbles are two key factors contributing to differences in velocity between samples of bubbly and bubble-free water. As depicted in Fig. 3, the velocity in bubble-free ice was found to be 4.5% higher than in bubbly ice, when measured by the same group at a frequency of 5 MHz and temperature of −18 °C. This disparity is likely attributed to an increase in path length due to scattering from the bubbles in bubbly samples.
3) *Dispersion:*
Sound velocity may vary with frequency, described as dispersion [40], [85]. Although dispersion is negligible in water above 0 °C [86], it is known to be important in ice at subzero temperatures [87]. Therefore, given the frequencies used for measurements ranged from 108 kHz to 10 MHz in Table I, the effect on sound velocity cannot be ignored. Accordingly, it is noted that the sound velocity in ice measured at 108 kHz is lower than measured at 2.25 MHz over all temperature between −20 °C and 0 °C.
4) *Crystal Orientation:*
Predominantly, the ice present in the biosphere, including ice used in these studies produced by air cryostat cooling and one-sided plate cooling, is ice 1_h with a hexagonal crystal structure [88]. The sound velocity in ice 1_h is contingent upon the angle between the direction of sound propagation and the crystallization orientation: the sound velocity varied from 3680 to 3780 m/s for angles between 0° and 90° in the studies of pure-water ice measurements (refer to study index (12) in Fig. 3) [62].
5) *Measurement Method:*
Different methodologies were employed across the studies displayed in Fig. 3, leading to potential systematic and experimental variations. These differences extend to the acoustic setup, calculation methods, freezing protocols, and techniques for thermal monitoring and insulation. Details of the methodologies are cataloged in Tables II and III. For example, although all studies used TOF for sound velocity calculation, time picking criteria varied: studies [2, 6] selected waveform onset, while studies [5, 7, 11] used peak criteria [55], [57], [61]. These discrepancies may contribute to the observed difference in measurements [89].

All of the factors listed here may contribute to the variations between measured sound velocity in Fig. 3. Some of these factors apply equally to longitudinal velocity data presented in Sections III-B–III-F collected from aqueous solutions, oils, and tissues with varying compositions of water and lipids, as well as to the measurement of shear velocity and attenuation coefficients.

B. Longitudinal Velocity of Aqueous Solution

Aqueous solutions, particularly saline solutions, are indispensable to human physiology and biological tissue function, as they facilitate nutrient transport, metabolic reactions, maintenance of pH balance, and help in preserving cell membrane integrity. Fig. 4(a) presents measurements of the longitudinal velocity of various aqueous solutions, including fresh water, NaCl solutions, and orange juice, measured over a temperature range of −40 °C to 20 °C and frequencies from 219 kHz to 5 MHz. To clarify, fresh water is water that can be found in nature, such as in glaciers and lakes, with a salinity level of less than 0.05% [90]. The longitudinal velocity of distilled water measured at 2.25 MHz [52] is provided for comparison, as well as an expanded view plot of the velocity above 0 °C.

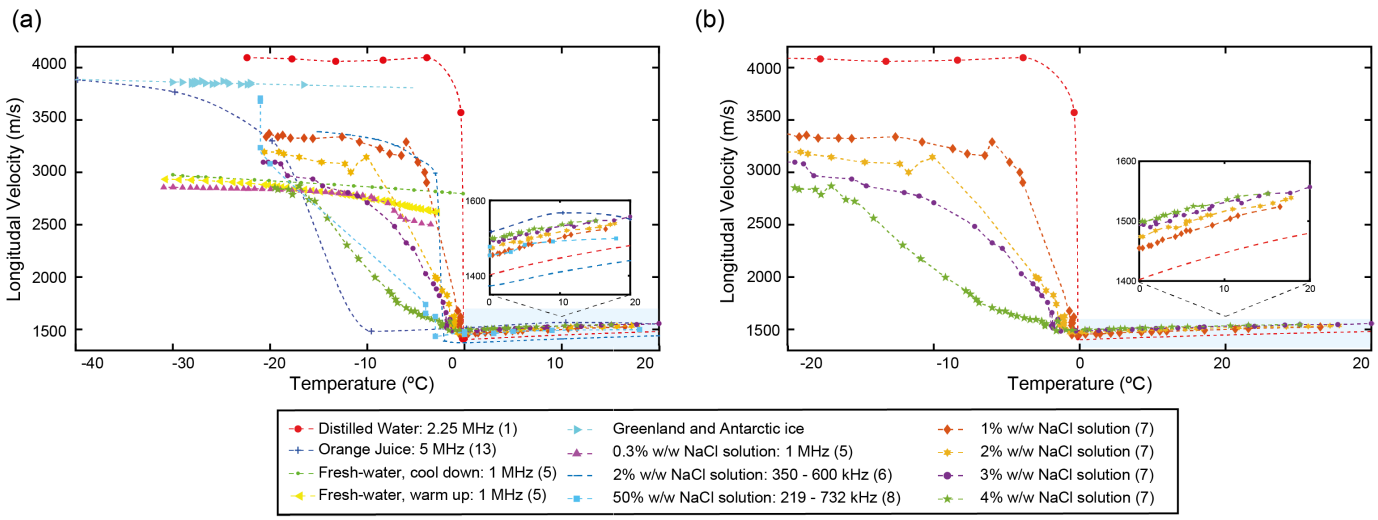

Fig. 4. (a) Longitudinal velocity versus temperature of aqueous solution during freezing. 1%–4% (w/w) NaCl solution were plotted separately in (b), with a larger view of above 0 °C. Points denote measurements, and curves show the trend. The sample materials and their measured frequencies are described in the legend; the number in brackets is the study index used in Tables I–III for comprehensive measurement information. Markers in the figure represent data sourced from original studies. Fit curves for study index (1) above 0 °C, and Greenland and Antarctic ice were based on equations from the original studies. For study index (1) below 0 °C, and study indices (5, 6, 7, 8, 13), the curves were derived using piecewise cubic Hermite interpolation [79].

Similar to water, the longitudinal velocity of aqueous solutions increases rapidly during the transition from liquid to solid state due to freezing [Fig. 4(a)], although this transition zone spans a wider range of temperatures. The longitudinal velocity of all collected aqueous solutions after freezing is lower than that of pure-water ice. Conversely, above 0 °C, the longitudinal velocities of the aqueous solutions are higher than that of pure water, except for the velocity of 2% NaCl solution, which is lower. In Fig. 4(a), it can be seen that the freezing point of each solution can be estimated from the rapid increase in longitudinal velocity. For all the aqueous solutions, the temperatures at which this rapid increase in longitudinal velocity occurs is below 0 °C. This change in longitudinal velocity due to the freezing demonstrates the phenomenon known as freezing point depression (FPD) [91], [92], where the freezing point of an aqueous solution is lower than for pure water.

The diversity of samples in Fig. 4(a), which include orange juice, fresh-water, sea-ice, and NaCl solutions of varying concentrations, in conjunction with the assortment of measurement methods used, introduces complexity when attempting to ascertain the impact of solute concentrations on longitudinal velocity. To counteract this issue and facilitate a clearer understanding, Fig. 4(b) separately plots the longitudinal velocities of specific NaCl concentrations [1%–4% (w/w)] obtained from a single study [57]. In the same vein, the longitudinal velocity of distilled water is plotted for comparison [52]. This is accompanied by an expanded view plot of the velocity measurements above 0 °C to aid comprehension of the effect of NaCl concentration, one of the principal solutes in biological cells [93], on longitudinal velocity.

Fig. 4(b) shows that during the freezing period, the increase in longitudinal velocity is faster and sharper with decreasing salinity. For lower salinity solutions, the longitudinal velocity has its minimum at higher temperatures, and increases more rapidly for temperatures below this. This corresponds to two physical phenomena: the added salt in pure water depresses the freezing point (FPD) [94], and slows down the ice nucleation process [95]. Conversely, above freezing temperature, the velocities recorded for all saline solutions exceed those of pure water. The data appear to show a trend of increasing velocity with increased salinity, however, the observed differences are small. It remains uncertain whether these differences are statistically significant, since measurement uncertainty was not quantified in the original study.

These findings offer essential insights into the effects of salinity on the velocity profiles of these solutions, which is useful in the interpretation of ultrasound measurements in biological and environmental contexts. However, to establish a more precise understanding of the relationship between solute concentration and longitudinal velocity during freezing, additional experimental data and comprehensive studies will be required.

C. Longitudinal Velocity of Lipids

Lipids are of importance to the human body and biological organisms, integral to cellular structure, energy reserves, and molecular signaling processes. Fig. 5 shows the longitudinal velocity of different types of lipid, including olive oil, corn oil, lard (pork fat), and dripping (beef fat), plotted against temperature. These measurements were acquired by Miles et al. [59], with the same methods used for all measurements.

Much like water, the longitudinal velocity of fats and oils also demonstrates an upward trend as temperature drops from 110 °C to −50 °C, rising from 1180 to 2100 m/s (a 78% increase). However, this change is much more gradual, and smoother in comparison to the dramatic 189% surge during the phase transition for water. This suggests that while fats and oils do undergo changes in acoustic properties with temperature, these shifts do not exhibit the sharp discontinuities

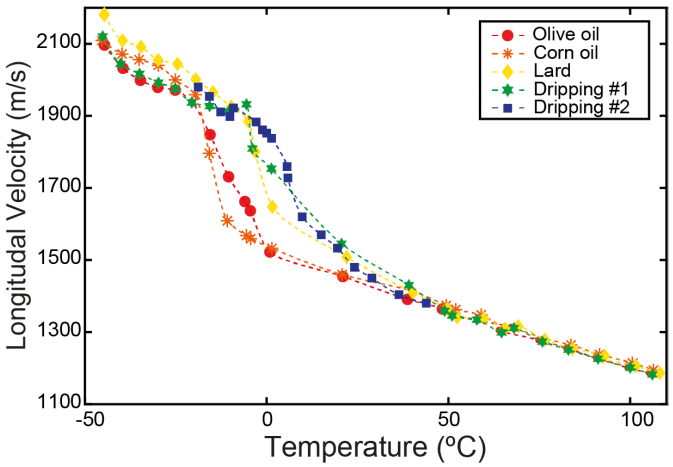

Fig. 5. Longitudinal velocity versus temperature of lipid, including vegetable oil and animal fat. For comprehensive measurement information, see study index (9) in Tables I–III. Markers in the figure represent data sourced from original studies. Fitting curves were derived using piecewise cubic Hermit interpolation [79] .

characteristic of the water-to-ice phase transition. However, the velocity increase in lipids during phase transition is considerably more marked than changes brought about solely by temperature variations in either solid or liquid states. For instance, for olive oil, the slope of longitudinal velocity during the phase transition which appears to occur between −20 °C and 2 °C is roughly six times greater than in the liquid phase between 2 °C and 100 °C, and three times that of the solid phase between −50 °C and −20 °C. At temperatures above 2 °C, the rate of change is −3.2 m/(s·°C); this rate increases to −19.1 m/(s·°C) between −20 °C and 2 °C during phase transition; and slows to −6.3 m/(s·°C) at temperatures below −20 °C in the solid phase. This effect is less distinct for the animal fats tested which exhibit smaller changes in rate of sound velocity increase, potentially due to the type of bonds within the fat [96]. The phase change also occurs at higher temperatures for these animal fats compared to the vegetable oils tested. The above analysis emphasizes the distinctive acoustic behavior of lipids during phase transitions compared to water, which might be due to the higher viscosity of lipid [97], [98].

D. Longitudinal Velocity of Biological Tissues

The constituent elements of tissues, such as water, lipids, and proteins, are present in different proportions across various tissues. For instance, human adipose tissue is predominantly lipid-rich, averaging 71.4% lipid content. In contrast, normal human liver tissue contains a relatively minuscule amount of lipid, just 0.3% on average [29]. These differences in composition significantly influence the unique characteristics and functions of each tissue type. Miles and Cutting [20] and Miles and Fursey [60] measured the acoustic properties of tissues with varying water-to-fat ratios over a temperature range of −20 °C to 40 °C [see Fig. 6(a)]. The samples included lean beef with a 70.2% water proportion, beef muscles with different water and fat contents, and bovine adipose tissue with up to 74.3% lipid. All the beef samples were minced to ensure homogeneity. The measurements presented in Figs. 5 and 6(a) were obtained using the same method by Miles and Cutting [20], Miles et al. [59], and Miles and Fursey [60].

Fig. 6(a) illustrates that the longitudinal velocity of tissues with different composition ratios of water and lipid diverges both below and above 0 °C. The range of measured velocities of the different samples is 4.7× greater in the subzero range than above 0 °C. Specifically, above 0 °C, the longitudinal velocity of all tissues are similar, ranging from 1435 to 1665 m/s, with a difference of 230 m/s across the temperature range of 0 °C to 40 °C. Conversely, below 0 °C, the velocity ranges from 2010 and 3090 m/s, exhibiting substantial differences up to 1080 m/s between tissue samples within the temperature range of −20 °C to 0 °C.

Additionally, the change in velocity with tissue composition exhibits contrasting tendencies below and above 0 °C. Below 0 °C, the velocity of tissue increases as the water concentration rises (or fat concentration declines) for all the measured tissues. On the other hand, above 0 °C, the velocity of lean beef, which has the highest water concentration among the samples, increases with temperature. In contrast, the velocity of adipose tissue, which has the lowest percentage of water, decreases as the temperature rises in the temperature domain above 0 °C.

The velocity in tissues with different composition ratios of water and lipids lies between the velocities of pure water and lipids. To highlight the variations in velocity with water/fat composition, Fig. 6(b) combines data from water (Fig. 3), and lipid samples (Fig. 5) with those from different tissue samples with various water/lipid ratios [Fig. 6(a)]. The velocity ranges of water, spanning from 3595 to 4095 m/s, and lipids, ranging from 1559 to 2045 m/s at temperatures below 0 °C, set the bounds for tissue velocities. This pattern is not observed at temperatures above 0 °C, where the velocity ranges overlap. This larger range of velocities below 0 °C compared to those above 0 °C may arise due to larger changes in stiffness in water on freezing compared to the solidification of lipids [99], [100], [101].

Below 0 °C, the velocity variation between tissue samples is governed by the water-to-lipid ratio. As observed previously, the velocity increases with rising water content and falls with increased lipid content [see arrows in Fig. 6(b)]. The composition of tissue plays a critical role in determining its acoustic properties. Further studies are necessary to uncover the mechanisms by which the velocity of tissues is regulated in a broader range of tissue types.

E. Shear Wave Velocity

As liquid transitions to solid during freezing, its shear strength increases, thereby facilitating the propagation of shear waves [102]. In the field of medical ultrasound, shear waves are instrumental in evaluating tissue elasticity, which is used in the diagnosis of various pathological conditions [103], [104]. Fig. 7 collects the measured shear wave velocities of frozen liquids, including bubble-free ice, fresh-water ice, NaCl solution ice, and orange juice ice. Measurements span frequencies from 108 kHz to 5 MHz, and temperatures from −50 °C to 0 °C.

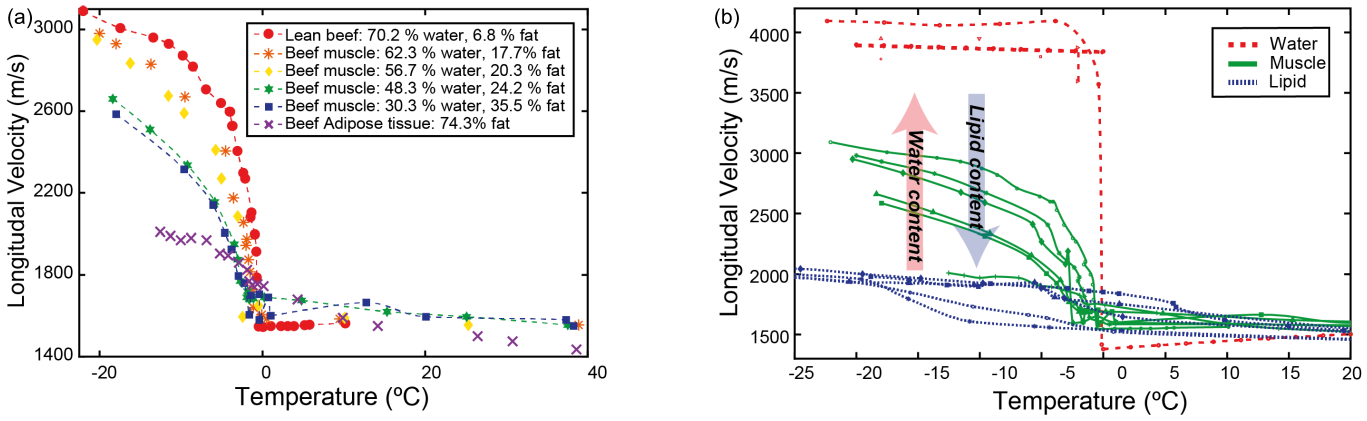

Fig. 6. (a) Longitudinal velocity versus temperature of tissues with different mixtures of water and fat. For comprehensive measurement information, see study index (9) in Tables I–III. Markers in the figure represent data sourced from original studies. Fit curves were derived using piecewise cubic Hermite interpolation [79]. (b) Comparative analysis of longitudinal velocity in muscle tissues. Data from pure water in Fig. 3, lipid in Fig. 5, and varied water/lipid compositions in (a) illustrate velocity shifts in relation to muscle tissue composition.

The shear wave velocity of frozen pure water and aqueous solutions measured between −50 °C and 0 °C ranges from 1560 to 2200 m/s, which is lower than the measured longitudinal velocity of these samples below 0 °C. Comparing longitudinal and shear velocities measured in one study (2) [53] (see Table I), the average shear velocity of bubble-free ice at −20 °C was measured to be 1855 m/s, nearly 50% slower than the longitudinal velocity of 3888 m/s.

Additionally, the shear velocity of ice significantly exceeds the values measured for tissues or tissues phantoms at ambient temperature. For instance, the shear velocity of bovine muscle ranges from 3.8 to 7.2 m/s [105], with even lower velocities used to represent liver in tissue phantoms, ranging from 1.0 to 2.0 m/s across various stiffness settings [106]. The noticeable increase in shear velocities at low temperatures is primarily attributed to the enhanced shear stiffness of samples after being frozen [107], [108]. Shear waves are not supported in water due to the insufficient shear modulus and strain [109]. However, a direct comparison in shear velocities at ambient temperature and at low temperature is precluded by the lack of available data from biological tissues at low temperatures.

The shear velocity of frozen liquids tends to increase as temperature decreases. However, comparison of these data can be complex due to the wide temperature range covered by the measurements and limited number of datasets. For instance, within the temperature range of −20 °C to 0 °C, the shear velocity of bubble-free ice and fresh-water ice is far lower than that of a 3% (w/w) NaCl solution. The measured shear velocity of sea ice, however, fluctuates significantly within the temperature range of −20 °C to 0 °C [55]. The measured longitudinal velocity for this sample [study index (5)] suggests that freezing occurs at approximately −8 °C. This finding may account for the observed variation in shear velocity between −8 °C and 0 °C, however, the reason for continued changes in shear velocity beyond this point are not clear, but it should be noticed that shear velocity measurements typically have higher uncertainties. The shear velocity of the fresh-water ice measured during both freezing and thawing exhibits only minor differences, in contrast to those observed in longitudinal

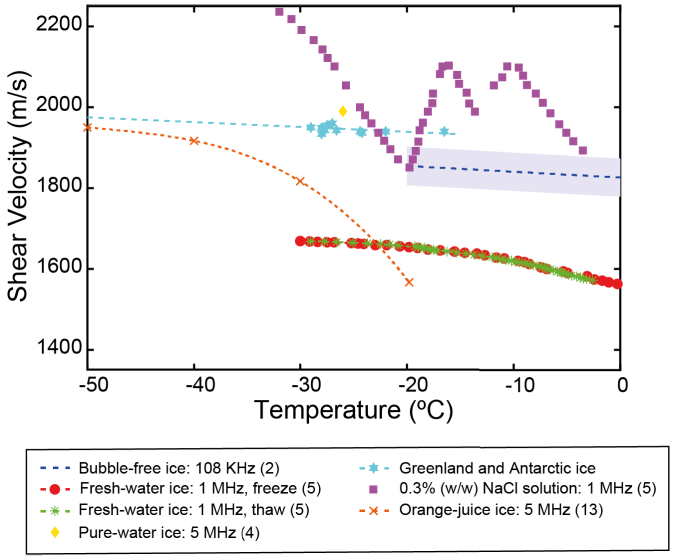

Fig. 7. Shear velocity versus temperature of water-ice and frozen aqueous solution. The sample materials and their measured frequencies are described in the legend; the number in brackets is the study index used in Tables I–III. Markers in the figure represent data sourced from original studies. Fit curves for study index (2) and Greenland and Antarctic ice were based on equations from the original studies. For study index (5, 13), the curves were derived using piecewise cubic Hermite interpolation [79]. The shading of the fit curve for bubble free ice [study index (2)] represents the measurement uncertainty defined by the calculation of standard deviation from the original study.

velocity during freeze-thaw cycles [55]. Additionally, the change in shear velocity is not linear with temperature.

Uncertainty in shear velocity measurements is significant and typically exceeds that associated with longitudinal velocity. Although the system setup and calculation principles for measuring both velocities are the same, shear waves propagate at lower speeds and shear attenuation is typically higher [110]. Due to the low velocity of shear waves [111], there is a higher possibility that shear waves will become combined with other waveforms, such as waves reflected from boundaries. Additionally, due to the high attenuation, shear waves may be too weak to be detected, and difficult to distinguish from

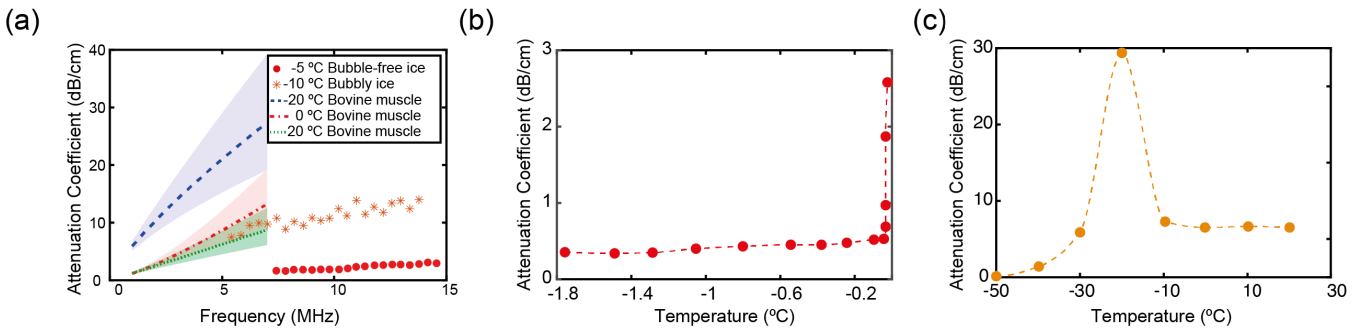

Fig. 8. (a) Attenuation coefficient versus frequency of water-ice, and bovine skeletal muscle (post rigor bovine) below 0 °C [study index (11)]. Attenuation coefficient versus temperature of (b) pure-water ice measured at 25 MHz [study index (12)] and (c) orange juice-ice measured at 5 MHz [study index (13)]. Markers in the figure represent data sourced from original studies. Fit curves for the attenuation coefficient of bovine muscle shown in (a) were based on equations from the original studies. The curves in (b) and (c) were fit using piecewise cubic Hermite interpolation [79]. The shading of the fit curves in (a) represent the measurement uncertainty defined by the calculation of standard deviation in the original study.

noise [112]. This all must be considered when measuring shear velocity. Thus, while shear wave measurements offer valuable insights, they necessitate careful interpretation and analysis due to the inherent complexities.

F. Attenuation Coefficient

The attenuation coefficient, an important acoustic property, plays a crucial role in ultrasound applications by quantifying the decrease in the intensity of ultrasound waves as they propagate through different materials. In Fig. 8, the measured attenuation coefficients of various samples at temperatures below 0 °C are presented, demonstrating their frequency and temperature dependence. Specifically, Fig. 8(a) displays the attenuation coefficients of bubbly and bubble-free ice, and bovine skeletal muscle samples as a function of frequency, while Fig. 8(b) and (c) depicts the temperature-dependent attenuation coefficients of pure water and orange juice at 25 and 5 MHz, respectively.

In Fig. 8(a), the attenuation coefficients of water-ice and muscle samples both exhibit a linear increase with rising frequency. Bubbly ice has a higher attenuation coefficient than bubble-free ice samples between 7 and 15 MHz. This difference, however, may not be solely attributable to the bubble content of the samples, although higher bubble concentrations do increase the attenuation coefficient through increased scattering [113], [114]. These samples were measured at different temperatures (−10 °C for bubbly ice and −5 °C for bubble-free ice), making direct comparisons challenging.

The relationship between the attenuation coefficient and temperature can be further explored for bovine skeletal muscle, with the ultrasonic wave propagation parallel to the fiber direction. The attenuation coefficient of the muscle samples increased with declining temperature. The increase in attenuation at −20 °C compared to 0 °C is more pronounced than the difference between measurements obtained at 0 °C and 20 °C. There may be some contribution to this increased attenuation coefficient from the water content in bovine muscle, as the attenuation coefficient of water increases from 0.5 to 2.8 dB/cm at 25 MHz once frozen, as shown in Fig. 8(b). The data in Fig. 8(b) further shows that attenuation may be significantly increased during the phase transition. However, the data for attenuation in ice covers an extremely small temperature range, and it is far lower than the measured attenuation coefficient in the tissue.

The attenuation coefficient of orange juice [Fig. 8(c)] peaks at 30 dB/cm at −20 °C and at 5 MHz, which corresponds to the temperature of the phase transition zone which can be observed by the increase in sound velocity in Fig. 4(a). Above the transition zone temperature, the attenuation coefficient increases from 6.5 to 7.3 dB/cm at 5 MHz as the temperature decreases from 20 °C to −10 °C. The attenuation coefficient then peaks during freezing, marking a fourfold increase compared to that at 20 °C. Following this peak, the attenuation coefficient drops to 8 dB/cm at −30 °C and continues to decrease as the temperature falls further, indicating that the phase transition is completed.

The spike in the attenuation coefficient of both water and orange juice may be attributed to ice nucleation and partial freezing during the phase transition from liquid to solid. The mechanism underlying waveform attenuation during phase transition is still an open question [115], [116], [117]. As mentioned in Section II-A, waveform attenuation results from the combined effects of absorption and scattering during waveform propagation within materials. Their relative contributions to waveform attenuation, however, are not well-defined. Further measurements and studies on this topic are warranted.

IV. Discussion and Summary

The acoustic properties of biological materials at low temperatures are not only fundamental to existing medical applications such as ultrasound-guided cryosurgery [21], but also for novel and emerging applications, such as tissue rewarming after cryopreservation [26], [27]. However, existing data are very limited, and are dispersed across a range of scientific fields, from seismology to glaciology and the food industry. The lack of a consolidated resource poses a considerable challenge for researchers in this area. We aimed to address this issue by gathering and analyzing these data on the low-temperature longitudinal and shear velocity and attenuation coefficients of biological tissues and related substances, including water, aqueous solutions, and lipids. Furthermore, the methods and conditions used for each measurement were

compared in this review, generating insights which should serve as a useful foundation for those seeking to conduct similar experiments. More importantly, the compilation of the measurements methods employed at low-temperatures holds the potential to increase standardization and help in improving the accuracy and reliability of measurements obtained in different applications of ultrasound.

On reviewing the previously published studies on low-temperature acoustic properties in terms of their methods and results, several further questions arise. The limited measurement data, differences in measurement methods, and limited quantification of measurement uncertainties in general calls for further investigation of the low-temperature ultrasonic properties of materials. Due to the limited number of samples, shear wave propagation at low temperatures is less well quantified compared to the longitudinal velocity. Among the available data, the compositions of the samples vary from naturally existing fresh water, to pure water, and lab-made NaCl solutions of different concentrations, with measurements made using different setups and calculation methods, and different frequencies across the studies, as summarized in Tables II and III. The studies covered in this review were conducted between 1976 and 2021, with physical sample sizes ranging from millimeters to meters, and frequencies ranging from kilohertz to megahertz (see Table I).

Although PES and TTS setups are acoustically equivalent for the frequency-independent velocity and attenuation coefficient measurement, any systematic differences between the SIM and MRM calculation methods have not been evaluated either practically or theoretically. The measurement uncertainty for MRM can be large, arising from sources including the size and length of the buffer rod, surface roughness, and parallelism [47]. To assess the influence on measurement uncertainty of the methods used in different studies, and to facilitate comparison of results, validation of the measurement system using a reference or standard sample with known acoustic properties if possible is suggested [4]. For low-temperature samples, however, it may be difficult to exclude the influence of temperature gradients and volume expansion during freezing even with reference samples. Water increases in volume by almost 10% during freezing [118]. Depending on the setup, the path distance of the signal may therefore increase, which if not accounted for, will reduce the accuracy of sound velocity and attenuation coefficient measurements.

Additionally, the temperature gradients in low-temperature samples must be considered. Both SIM and MRM are sensitive to temperature gradients [47], which are dependent on sample volume, thickness, and freezing protocol. As mentioned in Section II-C2, the temperature of samples frozen by one-sided cooling is lower on the side contacting the freezing plate, however, for samples frozen by air-cooling, the temperature will be lower at the edges than the center. The effect of temperature gradients and volume expansion during freezing requires further experimental evaluation, and their contribution to the measurement uncertainties should be assessed.

In addition to the measurement uncertainties already discussed, the stability of acoustic properties over time when samples are held at a certain temperature is still a question. The velocity of brine ice with a 50% (w/w) NaCl concentration rose from 3236 to 3709 m/s after two weeks of freezer storage at −21 °C [58] (Fig. 3). Additionally, a 7% difference was observed in the longitudinal velocity of fresh water at −3 °C between measurements made during freezing and thawing cycles [55] (Fig. 3). Differences in acoustic properties in relation to storage period and freeze-thaw cycles may be influenced by the ice content, structure, and distribution throughout the freezing process. For example, Azuma et al. [119] highlighted that ice grain size expanded from 0.2 to 1.7 mm after a 35-day storage period. The interplay between the acoustic properties, storage period and freeze-thaw cycles is still an open question which requires further investigation.

REFERENCES

[1] R. Truell, C. Elbaum, and B. B. Chick, *Ultrasonic Methods in Solid State Physics*. New York, NY, USA: Academic, 2013.

[2] J. Blitz and G. Simpson, *Ultrasonic Methods of Nondestructive Testing*, vol. 259. Berlin, Germany: Springer, 1995.

[3] B. Lüthi, *Physical Acoustics in the Solid State*, vol. 148. Berlin, Germany: Springer, 2007.

[4] B. Zeqiri, W. Scholl, and S. P. Robinson, "Measurement and testing of the acoustic properties of materials: A review," *Metrologia*, vol. 47, no. 2, pp. S156–S171, Apr. 2010.

[5] W. T. Shi et al., "Subharmonic imaging with microbubble contrast agents: Initial results," *Ultrason. Imag.*, vol. 21, no. 2, pp. 79–94, 1999.

[6] F. Forsberg, J.-B. Liu, W. T. Shi, J. Furuse, M. Shimizu, and B. B. Goldberg, "In vivo pressure estimation using subharmonic contrast microbubble signals: Proof of concept," *IEEE Trans. Ultrason., Ferroelectr., Freq. Control*, vol. 52, no. 4, pp. 581–583, Apr. 2005.

[7] K. Kalayeh et al., "Pressure measurement in a bladder phantom using contrast-enhanced ultrasonography—A path to a catheter-free voiding cystometrogram," *Investigative Radiol.*, vol. 58, no. 3, pp. 181–189, 2023.

[8] K. Kalayeh, J. B. Fowlkes, J. Claflin, M. L. Fabiilli, W. W. Schultz, and B. S. Sack, "Ultrasound contrast stability for urinary bladder pressure measurement," *Ultrasound Med. Biol.*, vol. 49, no. 1, pp. 136–151, 2023.

[9] J. C. Bamber and C. R. Hill, "Ultrasonic attenuation and propagation speed in mammalian tissues as a function of temperature," *Ultrasound Med. Biol.*, vol. 5, no. 2, pp. 149–157, Jan. 1979.

[10] B. M. Howe, J. Miksis-Olds, E. Rehm, H. Sagen, P. F. Worcester, and G. Haralabus, "Observing the oceans acoustically," *Front. Mar. Sci.*, vol. 6, p. 426, Jul. 2019.

[11] K. Ono, "A comprehensive report on ultrasonic attenuation of engineering materials, including metals, ceramics, polymers, fiber-reinforced composites, wood, and rocks," *Appl. Sci.*, vol. 10, no. 7, p. 2230, 2020.

[12] K. J. Parker, "Ultrasonic attenuation and absorption in liver tissue," *Ultrasound Med. Biol.*, vol. 9, no. 4, pp. 363–369, 1983.

[13] M. Bakaric, P. Miloro, A. Javaherian, B. T. Cox, B. E. Treeby, and M. D. Brown, "Measurement of the ultrasound attenuation and dispersion in 3D-printed photopolymer materials from 1 to 3.5 MHz," *J. Acoust. Soc. Amer.*, vol. 150, no. 4, pp. 2798–2805, Oct. 2021.

[14] B. E. Treeby, E. Z. Zhang, A. S. Thomas, and B. T. Cox, "Measurement of the ultrasound attenuation and dispersion in whole human blood and its components from 0–70 MHz," *Ultrasound Med. Biol.*, vol. 37, no. 2, pp. 289–300, 2011.

[15] X. Cheng, M. Zhang, B. Xu, B. Adhikari, and J. Sun, "The principles of ultrasound and its application in freezing related processes of food materials: A review," *Ultrason. Sonochem.*, vol. 27, pp. 576–585, Nov. 2015.

[16] R. J. Hansman Jr and M. S. Kirby, "Measurement of ice accretion using ultrasonic pulse-echo techniques," *J. Aircr.*, vol. 22, no. 6, pp. 530–535, 1985.

[17] H. Kohnen, "The temperature dependence of seismic waves in ice," *J. Glaciol.*, vol. 13, no. 67, pp. 144–147, 1974.

[18] S. Hellmann et al., "Acoustic velocity measurements for detecting the crystal orientation fabrics of a temperate ice core," *Cryosphere*, vol. 15, no. 7, pp. 3507–3521, Jul. 2021.

[19] D. Shore, M. Woods, and C. Miles, "Attenuation of ultrasound in post rigor bovine skeletal muscle," *Ultrasonics*, vol. 24, no. 2, pp. 81–87, 1986.

[20] G. A. Miles and G. L. Cutting, "Technical note: Changes in the velocity of ultrasound in meat during freezing," *Int. J. Food Sci. Technol.*, vol. 9, no. 1, pp. 119–122, Mar. 1974.

[21] M. Karthikeyan et al., "Modern applications of cryosurgery in oncology," *Global J. Cancer Therapy*, vol. 6, no. 1, pp. 010–014, 2020.

[22] G. Onik, C. Cooper, H. I. Goldberg, A. A. Moss, B. Rubinsky, and M. Christianson, "Ultrasonic characteristics of frozen liver," *Cryobiology*, vol. 21, no. 3, pp. 321–328, Jun. 1984.

[23] W. Kimmig, R. Hicks, and E. W. Breitbart, "Ultrasound in cryosurgery," *Clinics Dermatol.*, vol. 8, no. 1, pp. 65–68, Jan. 1990.

[24] M. J. Taylor, B. P. Weegman, S. C. Baicu, and S. E. Giwa, "New approaches to cryopreservation of cells, tissues, and organs," *Transfusion Med. Hemotherapy*, vol. 46, no. 3, pp. 197–215, 2019.

[25] P. Kilbride et al., "Cryopreservation and re-culture of a 2.3 litre biomass for use in a bioartificial liver device," *PLoS ONE*, vol. 12, no. 8, Aug. 2017, Art. no. e0183385.

[26] A. Olmo, P. Barroso, F. Barroso, and R. Risco, "The use of high-intensity focused ultrasound for the rewarming of cryopreserved biological material," *IEEE Trans. Ultrason., Ferroelectr., Freq. Control*, vol. 68, no. 3, pp. 599–607, Mar. 2021.

[27] R. Xu, B. E. Treeby, and E. Martin, "Experiments and simulations demonstrating the rapid ultrasonic rewarming of frozen tissue cryovials," *J. Acoust. Soc. Amer.*, vol. 153, no. 1, pp. 517–528, Jan. 2023.

[28] L. W. Thomas, "The chemical composition of adipose tissue of man and mice," *Quart. J. Exp. Physiol. Cognate Med. Sci., Transl. Integr.*, vol. 47, no. 2, pp. 179–188, 1962.

[29] F. A. Duck, *Physical Properties of Tissues: A Comprehensive Reference Book*. London, U.K.: Academic Press, 1990, ch. 9, pp. 319–328.

[30] C. Gabriel and A. Peyman, "Dielectric properties of biological tissues; variation with age," in *Conn's Handbook of Models for Human Aging*. London, U.K.: Elsevier, 2018, pp. 939–952.

[31] P. L. Privalov and C. Crane-Robinson, "Role of water in the formation of macromolecular structures," *Eur. Biophys. J.*, vol. 46, no. 3, pp. 203–224, Apr. 2017.

[32] Wikipedia. (2024). *Velocity*. Accessed: Feb. 26, 2024. [Online]. Available: https://en.wikipedia.org/wiki/Velocity

[33] R. S. C. Cobbold, *Foundations of Biomedical Ultrasound*. New York, NY, USA: Oxford Univ. Press, 2007.

[34] D. Marioli, C. Narduzzi, C. Offelli, D. Petri, E. Sardini, and A. Taroni, "Digital time-of-flight measurement for ultrasonic sensors," *IEEE Trans. Instrum. Meas.*, vol. 41, no. 1, pp. 93–97, Feb. 1992.

[35] L. Angrisani and R. Schiano Lo Moriello, "Estimating ultrasonic time-of-flight through quadrature demodulation," *IEEE Trans. Instrum. Meas.*, vol. 55, no. 1, pp. 54–62, Feb. 2006.

[36] M. R. Hoseini, X. Wang, and M. J. Zuo, "Estimating ultrasonic time of flight using envelope and quasi maximum likelihood method for damage detection and assessment," *Measurement*, vol. 45, no. 8, pp. 2072–2080, Oct. 2012.

[37] C. Li, L. Huang, N. Duric, H. Zhang, and C. Rowe, "An improved automatic time-of-flight picker for medical ultrasound tomography," *Ultrasonics*, vol. 49, no. 1, pp. 61–72, Jan. 2009.

[38] L. Brillouin, *Wave Propagation and Group Velocity*, vol. 152. New York, NY, USA: Academic, 2013.

[39] J. B. Molyneux and D. R. Schmitt, "First-break timing: Arrival onset times by direct correlation," *Geophysics*, vol. 64, no. 5, pp. 1492–1501, Sep. 1999.

[40] W. Sachse and Y.-H. Pao, "On the determination of phase and group velocities of dispersive waves in solids," *J. Appl. Phys.*, vol. 49, no. 8, pp. 4320–4327, Aug. 1978.

[41] C. R. Hill, J. C. Bamber, and G. R. ter Haar, *Physical Principles of Medical Ultrasonics*. Hoboken, NJ, USA: Wiley, 2004.

[42] K. A. Wear, "Measurements of phase velocity and group velocity in human calcaneus," *Ultrasound Med. Biol.*, vol. 26, no. 4, pp. 641–646, May 2000.

[43] V. A. Del Grosso and C. W. Mader, "Speed of sound in pure water," *J. Acoust. Soc. Amer.*, vol. 52, no. 5B, pp. 1442–1446, Nov. 1972.

[44] W. Marczak, "Water as a standard in the measurements of speed of sound in liquids," *J. Acoust. Soc. Amer.*, vol. 102, no. 5, pp. 2776–2779, Nov. 1997.

[45] J. Ablitt, "Technical guides–speed of sound in pure water," Nat. Phys. Laboartory, Teddington, U.K., Tech. Rep., 2000. [Online]. Available: http://resource.npl.co.uk/acoustics/techguides/soundpurewater/speedpw.pdf

[46] J. M. Pinkerton, "The absorption of ultrasonic waves in liquids and its relation to molecular constitution," *Proc. Phys. Soc. B*, vol. 62, no. 2, p. 129, 1949.

[47] S. Hoche, M. A. Hussein, and T. Becker, "Ultrasound-based density determination via buffer rod techniques: A review," *J. Sensors Sensor Syst.*, vol. 2, no. 2, pp. 103–125, Jul. 2013.

[48] J. E. Carlson, J. van Deventer, A. Scolan, and C. Carlander, "Frequency and temperature dependence of acoustic properties of polymers used in pulse-echo systems," in *Proc. IEEE Symp. Ultrason.*, Oct. 2003, pp. 885–888.

[49] J. Carlson, J. van Deventer, and M. Micella, "Accurate temperature estimation in ultrasonic pulse-echo systems," in *World Congress on Ultrasonics: 07/09/2003-10/09/2003* (Institut Biomedical des Cordeliers). Paris, France: Université Pierre et Marie Curie, 2003, pp. 1565–1568.

[50] J. Martinsson, J. E. Carlson, and J. Niemi, "Model-based phase velocity and attenuation estimation in wideband ultrasonic measurement systems," *IEEE Trans. Ultrason., Ferroelectr., Freq. Control*, vol. 54, no. 1, pp. 138–146, Jan. 2007.

[51] J. Carlson, M. Nilsson, E. Fernández, and J. A. Planell, "An ultrasonic pulse-echo technique for monitoring the setting of $CaSO_4$-based bone cement," *Biomaterials*, vol. 24, no. 1, pp. 71–77, Jan. 2003.

[52] H. Sigfusson, G. R. Ziegler, and J. N. Coupland, "Ultrasonic monitoring of food freezing," *J. Food Eng.*, vol. 62, no. 3, pp. 263–269, May 2004.

[53] C. Vogt, K. Laihem, and C. Wiebusch, "Speed of sound in bubble-free ice," *J. Acoust. Soc. Amer.*, vol. 124, no. 6, pp. 3613–3618, Dec. 2008.

[54] A. C. Smith and D. Kishoni, "Measurement of the speed of sound in ice," *AIAA J.*, vol. 24, no. 10, pp. 1713–1715, Oct. 1986.

[55] X. Chang, W. Liu, G. Zuo, Y. Dou, and Y. Li, "Research on ultrasonic-based investigation of mechanical properties of ice," *Acta Oceanol. Sinica*, vol. 40, no. 10, pp. 97–105, Oct. 2021.

[56] J. Matsushima, M. Suzuki, Y. Kato, T. Nibe, and S. Rokugawa, "Laboratory experiments on compressional ultrasonic wave attenuation in partially frozen brines," *Geophysics*, vol. 73, no. 2, pp. N9–N18, Mar. 2008.

[57] C. Aparicio, L. Otero, B. Guignon, A. D. Molina-García, and P. D. Sanz, "Ice content and temperature determination from ultrasonic measurements in partially frozen foods," *J. Food Eng.*, vol. 88, no. 2, pp. 272–279, Sep. 2008.

[58] M. Prasad and J. Dvorkin, "Velocity and attenuation of compressional waves in brines," in *Proc. SEG Int. Expo. Annu. Meeting*. Richardson, TX, USA: OnePetro, 2004, pp. 1–4.

[59] C. A. Miles, G. A. J. Fursey, and R. C. D. Jones, "Ultrasonic estimation of solid/liquid ratios in fats, oils and adipose tissue," *J. Sci. Food Agricult.*, vol. 36, no. 3, pp. 215–228, Mar. 1985.

[60] C. A. Miles and G. A. J. Fursey, "Measurement of the fat content of meat using ultrasonic waves," *Food Chem.*, vol. 2, no. 2, pp. 107–118, Apr. 1977.

[61] Y. Liu, L. J. Bond, and H. Hu, "Ultrasonic-attenuation-based technique for ice characterization pertinent to aircraft icing phenomena," *AIAA J.*, vol. 55, no. 5, pp. 1602–1609, May 2017.

[62] J. Tamura, Y. Kogure, and Y. Hiki, "Ultrasonic attenuation and dislocation damping in crystals of ice," *J. Phys. Soc. Jpn.*, vol. 55, no. 10, pp. 3445–3461, Oct. 1986.

[63] S. Lee, L. J. Pyrak-Nolte, P. Cornillon, and O. Campanella, "Characterisation of frozen orange juice by ultrasound and wavelet analysis," *J. Sci. Food Agricult.*, vol. 84, no. 5, pp. 405–410, Apr. 2004.

[64] Wikipedia. (2023). *Ethanol*. Accessed: Aug. 11, 2023. [Online]. Available: http://en.wikipedia.org/wiki/Ethanol

[65] R. Kazys and V. Vaskeliene, "High temperature ultrasonic transducers: A review," *Sensors*, vol. 21, no. 9, p. 3200, May 2021.

[66] R. Kažys, A. Voleišis, and B. Voleišienė, "High temperature ultrasonic transducers," *Ultragarsas/Ultrasound*, vol. 63, no. 2, pp. 7–17, 2008.

[67] B. A. J. Angelsen, "A theoretical study of the scattering of ultrasound from blood," *IEEE Trans. Biomed. Eng.*, vol. BME-27, no. 2, pp. 61–67, Feb. 1980.

[68] K. G. Foote, "Discriminating between the nearfield and the farfield of acoustic transducers," *J. Acoust. Soc. Amer.*, vol. 136, no. 4, pp. 1511–1517, Oct. 2014.

[69] Wikipedia. (2023). *Thin Film*. Accessed: May 17, 2023. [Online]. Available: https://en.wikipedia.org/wiki/Thin_film

[70] I. Y. Kuo, B. Hete, and K. K. Shung, "A novel method for the measurement of acoustic speed," *J. Acoust. Soc. Amer.*, vol. 88, no. 4, pp. 1679–1682, Oct. 1990.

[71] W. McAdams, *Heat Transfer*, vol. 1, no. 51. New York, NY, USA: McGraw-Hill, 1954, p. 3.

[72] G. V. Barbosa-Cánovas, B. Altunakar, and D. J. Mejía-Lorío, *Freezing of Fruits and Vegetables: An Agribusiness Alternative for Rural and Semi-Rural Areas*, vol. 158. Rome, Italy: Food & Agriculture, 2005.

[73] A. Krasnoshlykov and V. I. Maksimov, "Experimental study of convective flows in the freezer," in *Proc. MATEC Web Conf.*, vol. 19, 2014, p. 01003.

[74] J. Saragusty, "Directional freezing for large volume cryopreservation," in *Cryopreservation and Freeze-Drying Protocols*. New York, NY, USA: Springer, 2015, pp. 381–397.

[75] A. Kumar, J. Prasad, N. Srivastava, and S. Ghosh, "Strategies to minimize various stress-related freeze–thaw damages during conventional cryopreservation of mammalian spermatozoa," *Biopreservation Biobanking*, vol. 17, no. 6, pp. 603–612, 2019.

[76] A. Arav and Y. Natan, "Directional freezing: A solution to the methodological challenges to preserve large organs," in *Seminars in Reproductive Medicine*. New York, NY, USA: Thieme Medical Publishers, 2009, pp. 438–442.

[77] C. Yeager and S. Courts, "A review of cryogenic thermometry and common temperature sensors," *IEEE Sensors J.*, vol. 1, no. 4, pp. 352–360, Dec. 2001.

[78] W. Su, J. Darkwa, and G. Kokogiannakis, "Review of solid–liquid phase change materials and their encapsulation technologies," *Renew. Sustain. Energy Rev.*, vol. 48, pp. 373–391, Aug. 2015.

[79] C. A. Rabbath and D. Corriveau, "A comparison of piecewise cubic Hermite interpolating polynomials, cubic splines and piecewise linear functions for the approximation of projectile aerodynamics," *Defence Technol.*, vol. 15, no. 5, pp. 741–757, Oct. 2019.

[80] A. H. Smith and A. W. Lawson, "The velocity of sound in water as a function of temperature and pressure," *J. Chem. Phys.*, vol. 22, no. 3, pp. 351–359, Mar. 1954.

[81] E. Hidalgo Baltasar, M. Taravillo, V. G. Baonza, P. D. Sanz, and B. Guignon, "Speed of sound in liquid water from (253.15 to 348.15) k and pressures from (0.1 to 700) MPa," *J. Chem. Eng. Data*, vol. 56, no. 12, pp. 4800–4807, Dec. 2011.

[82] G. S. Kell, "Effects of isotopic composition, temperature, pressure, and dissolved gases on the density of liquid water," *J. Phys. Chem. Reference Data*, vol. 6, no. 4, pp. 1109–1131, Oct. 1977.

[83] Wikipedia. (2023). *Distilled Water*. Accessed: May 22, 2023. [Online]. Available: https://en.wikipedia.org/wiki/Distilled_water

[84] R. A. Thuraisingham, "Sound speed in bubbly water at megahertz frequencies," *Ultrasonics*, vol. 36, no. 6, pp. 767–773, Apr. 1998.

[85] V. Mangulis, "Kramers-kronig or dispersion relations in acoustics," *J. Acoust. Soc. Amer.*, vol. 36, no. 1, pp. 211–212, Jan. 1964.

[86] E. L. Carstensen, "Measurement of dispersion of velocity of sound in liquids," *J. Acoust. Soc. Amer.*, vol. 26, no. 5, pp. 858–861, Sep. 1954.

[87] O. Conde, J. Leblond, and J. Teixeira, "Analysis of the dispersion of the sound velocity in supercooled water," *J. de Phys.*, vol. 41, no. 9, pp. 997–1000, 1980.

[88] Wikipedia. (2023). *Ice IH*. Accessed: May 22, 2023. [Online]. Available: https://en.wikipedia.org/wiki/Ice_Ih

[89] K. A. Wear et al., "Interlaboratory comparison of ultrasonic backscatter coefficient measurements from 2 to 9 MHz," *J. Ultrasound Med.*, vol. 24, no. 9, pp. 1235–1250, 2005.

[90] M. P. Stainton, M. J. Capel, and F. A. J. Armstrong, "The chemical analysis of fresh water," in *Fisheries and Environment Canada, Fisheries and Marine Services, Miscellaneous. Special Publication*, vol. 25, 2nd ed. 1977, p. 80.

[91] A. A. Zavitsas, "The nature of aqueous solutions: Insights into multiple facets of chemistry and biochemistry from freezing-point depressions," *Chem.–Eur. J.*, vol. 16, no. 20, pp. 5942–5960, 2010.

[92] C. P. Lamas, C. Vega, and E. G. Noya, "Freezing point depression of salt aqueous solutions using the Madrid-2019 model," *J. Chem. Phys.*, vol. 156, no. 13, 2022, Art. no. 134503.

[93] T. Morgan, "Effect of NaCl on composition and volume of cells of the rat papilla," *Amer. J. Physiol.-Renal Physiol.*, vol. 232, no. 2, pp. F117–F122, Feb. 1977.

[94] B. T. Doherty and D. R. Kester, "Freezing point of seawater," *J. Mar. Res.*, vol. 32, no. 2, pp. 285–300, 1974.

[95] S. Bauerecker, P. Ulbig, V. Buch, L. Vrbka, and P. Jungwirth, "Monitoring ice nucleation in pure and salty water via high-speed imaging and computer simulations," *J. Phys. Chem. C*, vol. 112, no. 20, pp. 7631–7636, May 2008.

[96] M. Bockisch, *Fats and Oils Handbook (Nahrungsfette und Öle)*. Amsterdam, The Netherlands: Elsevier, 2015, ch. 9.

[97] E. d. C. Andrade, "The viscosity of liquids," *Nature*, vol. 125, no. 3148, pp. 309–310, 1930.

[98] D. S. Viswanath, T. K. Ghosh, D. H. Prasad, N. V. Dutt, and K. Y. Rani, *Viscosity of Liquids: Theory, Estimation, Experiment, and Data*. Berlin, Germany: Springer, 2007, ch. 4.

[99] Q. Yin, E. Andò, G. Viggiani, and W. Sun, "Freezing-induced stiffness and strength anisotropy in freezing clayey soil: Theory, numerical modeling, and experimental validation," *Int. J. for Numer. Anal. Methods Geomech.*, vol. 46, no. 11, pp. 2087–2114, Aug. 2022.

[100] V. Anisimkin, V. Kolesov, A. Kuznetsova, E. Shamsutdinova, and I. Kuznetsova, "An analysis of the Water-to-Ice phase transition using acoustic plate waves," *Sensors*, vol. 21, no. 3, p. 919, Jan. 2021.

[101] L. Picas, F. Rico, and S. Scheuring, "Direct measurement of the mechanical properties of lipid phases in supported bilayers," *Biophys. J.*, vol. 102, no. 1, pp. L01–L03, Jan. 2012.

[102] Y. Zheng et al., "Shear wave propagation in soft tissue and ultrasound vibrometry," in *Wave Propagation Theories and Applications*. Rijeka, Croatia: InTech, Feb. 2013, doi: 10.5772/48629.

[103] R. M. S. Sigrist, J. Liau, A. E. Kaffas, M. C. Chammas, and J. K. Willmann, "Ultrasound elastography: Review of techniques and clinical applications," *Theranostics*, vol. 7, no. 5, pp. 1303–1329, 2017.

[104] X.-W. Cui et al., "Ultrasound elastography," *Endoscopic Ultrasound*, vol. 11, no. 4, p. 252, 2022.

[105] S. Chen et al., "Shearwave dispersion ultrasound vibrometry (SDUV) for measuring tissue elasticity and viscosity," *IEEE Trans. Ultrason., Ferroelectr, Freq. Control*, vol. 56, no. 1, pp. 55–62, Jan. 2009.

[106] M. L. Palmeri et al., "Radiological society of North America/quantitative imaging biomarker alliance shear wave speed bias quantification in elastic and viscoelastic phantoms," *J. Ultrasound Med.*, vol. 40, no. 3, pp. 569–581, Mar. 2021.

[107] A. Sawangsuriya, "Wave propagation methods for determining stiffness of geomaterials," in *Wave Processes in Classical and New Solids*. Rijeka, Croatia: InTech, Oct. 2012, doi: 10.5772/48562.

[108] M. Szarko, K. Muldrew, and J. E. Bertram, "Freeze-thaw treatment effects on the dynamic mechanical properties of articular cartilage," *BMC Musculoskeletal Disorders*, vol. 11, no. 1, pp. 1–8, Dec. 2010.

[109] M. Aziman, Z. Hazreek, A. Azhar, and D. Haimi, "Compressive and shear wave velocity profiles using seismic refraction technique," in *Proc. J. Phys., Conf.*, 2016, vol. 710, no. 1, Art. no. 012011.

[110] A. N. Norris, "An inequality for longitudinal and transverse wave attenuation coefficients," *J. Acoustic. Soc. Amer.*, vol. 141, no. 1, pp. 475–479, 2017.

[111] A. P. Sarvazyan, M. W. Urban, and J. F. Greenleaf, "Acoustic waves in medical imaging and diagnostics," *Ultrasound Med. Biol.*, vol. 39, no. 7, pp. 1133–1146, Jul. 2013.

[112] S. Crampin and Y. Gao, "A review of techniques for measuring shear-wave splitting above small earthquakes," *Phys. Earth Planet. Interiors*, vol. 159, nos. 1–2, pp. 1–14, Nov. 2006.

[113] S. Zhang et al., "Dynamic changes of integrated backscatter, attenuation coefficient and bubble activities during high-intensity focused ultrasound (HIFU) treatment," *Ultrasound Med. Biol.*, vol. 35, no. 11, pp. 1828–1844, Nov. 2009.

[114] L. A. Frizzell, E. L. Carstensen, and J. D. Davis, "Ultrasonic absorption in liver tissue," *J. Acoust. Soc. Amer.*, vol. 65, no. 5, pp. 1309–1312, May 1979.

[115] J. Matsushima, M. Suzuki, Y. Kato, and S. Rokugawa, "Estimation of ultrasonic scattering attenuation in partially frozen brines using magnetic resonance images," *Geophysics*, vol. 76, no. 1, pp. T13–T25, Jan. 2011.

[116] C. L. Hackert and J. O. Parra, "Estimating scattering attenuation from vugs or karsts," *Geophysics*, vol. 68, no. 4, pp. 1182–1188, Jul. 2003.

[117] A. Hosokawa and T. Otani, "Ultrasonic wave propagation in bovine cancellous bone," *J. Acoust. Soc. Amer.*, vol. 101, no. 1, pp. 558–562, Jan. 1997.

[118] M. Akyurt, G. Zaki, and B. Habeebullah, "Freezing phenomena in ice–water systems," *Energy Convers. Manage.*, vol. 43, no. 14, pp. 1773–1789, Sep. 2002.

[119] N. Azuma, T. Miyakoshi, S. Yokoyama, and M. Takata, "Impeding effect of air bubbles on normal grain growth of ice," *J. Struct. Geol.*, vol. 42, pp. 184–193, Sep. 2012.